

Flame front detection by active contour method from OH-PLIF images under microgravity

Yandong Tang (唐延东)¹, Yue Wang (王岳)², and Christian Eigenbrod³

¹Shenyang Institute of Automation, Chinese Academy of Sciences, Shenyang 110014

²Institute of Engineering Thermophysics, Chinese Academy of Sciences, Beijing 100080

³ZARM Institute, University of Bremen, Bremen 28359, Germany

Received March 9, 2006

It is difficult and high-cost to detect flame fronts by laser-sheet diagnostics under microgravity (μg), thus image processing is critical to obtain valuable information from the raw data. In the present study, premixed V-flames were detected under μg by OH planar laser-induced fluorescence (PLIF) and an effective method based on active contour model (ACM) is presented for automatic detecting and tracking flame fronts in the PLIF images. ACM can effectively detect the flame front in the images with low contrast and noises. Compared with other methods of flame front detection, the advantage of this method is that the image smoothing and image enhancement are not necessary for the correct detection of flame fronts in raw PLIF images.

OCIS codes: 100.0100, 120.0120.

The study of fluid physics influence on flame fronts is of fundamental importance for the design of more efficient and environmentally friendly combustion devices. The topology of flame fronts under μg provides a baseline for identifying buoyancy effects and analyzing dynamical behavior of premixed flames. However, applying laser-sheet diagnostics to visualize flame fronts in μg experiments is either difficult or high-cost[1]. In the present study, CH₄-air premixed V-flames were detected by applying OH planar laser-induced fluorescence (PLIF) technology under both normal gravity ($1g_0$) and microgravity (μg) in the Bremen drop tower[2]. Due to the difficulty of laser diagnostics as well as the high cost of μg experiments, the applied image processing techniques are critical to acquire valuable information from the resulting PLIF images. For further analysis of the data, such as the turbulence effect on flame surface geometry or the study of flame front development, the flame fronts in the PLIF images should be automatically and accurately detected and tracked with image processing.

A number of image segmentation methods have been used to get the contour of the flame in PLIF images for the detection of flame front[3]. In Ref. [4] the method of adaptive threshold was used to segment the flame front based on intensity histograms of the images. The adaptive threshold value can be also set by image gradients[5]. Nonetheless for low contrast and noisy PLIF images these methods are not always effective and sometimes the results are not acceptable. They still also suffer from the problems of determining the correct global or local thresholds in automatic processing the broad variety of images[3], and often result in contour gap and noise falsely detected as flame front boundary. Therefore, in these methods usually a post-processing procedure is necessary to distinguish the flame front boundary from other edge object in a PLIF image, and the contour gaps must be merged for further analyzing the buoyancy effects on premixed flames. In Ref. [3] the active contour model (ACM, known also as snake model) based on curve

evolution was used for the identification of flame front boundary. The snake model guarantees the continuity and smoothness of the detected contour or boundary. In the model a closed curve is initialized on the image and then allowed to evolve onto the image feature (e.g. edges of the object that we want to detect). In this method for the noise reduction the images were smoothed using non-linear anisotropic diffusion filter that smoothes out noise locally by diffusion flow. In principle this method relies on image gradients and the condition that the points in the flame front contour have higher intensity gradient. For some noisy PLIF images the condition is not always met.

For effective and automatic detection of flame fronts the active contour model based on region[6] was used in this paper. This method can detect objects whose boundaries are not necessarily defined by gradient of an image and no threshold value is used. Our experimental tests with the broad variety of PLIF images showed that the method is very effective for automatic flame front detection, especially for low contrast and noisy images. Also it is not needed to smooth the raw image, even if it is very noisy and in this way, the contours of flame front are very well detected and preserved.

Laser diagnostics of the V-flames is shown in Fig. 1. A

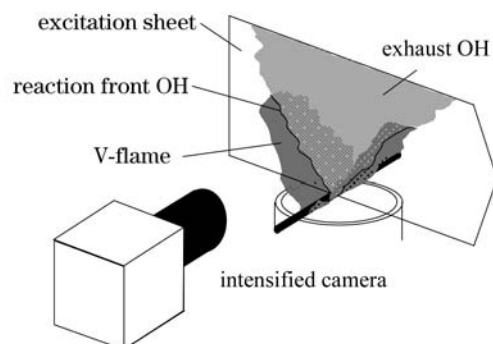


Fig. 1. Detecting flame fronts by OH-PLIF.



Fig. 2. An OH-PLIF image of a V-flame.

KrF laser of 248-nm wavelength was fixed on the top of the drop tower and the light beam followed the dropping capsule to provide light source of diagnostics. Inside the capsule the light beam was a sheet thinner than 0.5 mm. A pointing assembly in the capsule adjusted the laser beam to hold the position of the light sheet relative to the flame. The light sheet penetrated the flame and OH radicals in the product were excited to emit fluorescence. Thus the two-dimensional (2D) flow fields of the flames were visualized and the boundaries of illuminated and dark regions in the recorded images are flame fronts (see in Fig. 2).

Quality of the images was mainly influenced by the following factors: 1) instability of the laser induced the variation of light emission; 2) intensity distribution over the cross section of the laser beam led to inhomogeneous backgrounds; 3) decay of light intensity during drop; 4) movement of the mirrors of the pointing assembly changed optical path and hence influenced the intensity of light; 5) variant OH concentration along the flame fronts led to uneven contrast.

Due to the wide variety of image contrast along the flame edge, some image segmentation methods based on adaptive threshold and image gradients were tested and found to fail in automatic detection of flame fronts within large amounts of PLIF images.

Chan *et al.*^[6] proposed a model (C-V model) for active contour to detect objects in an image, based on techniques of curve evolution, and level sets. Unlike the classic active contour based on the gradient of a given image, the C-V model can detect the contours both with and without gradient. The interior contours are automatically detected, and the initial curve can be anywhere in the image.

Let C be the evolving curve, u_0 be the grey intensity of the image, and c_1, c_2 be the intensity averages of inside and outside of C , respectively. A fitting energy function is as

$$\begin{aligned} \text{Fit} = F_1(C) + F_2(C) &= \int_{\text{inside}(C)} |u_0(x, y) - c_1|^2 dx dy \\ &+ \int_{\text{outside}(C)} |u_0(x, y) - c_2|^2 dx dy. \end{aligned} \quad (1)$$

Assume that the image u_0 is formed by two regions of approximatively piecewise-constant intensities. Assume further that the object to be detected is one of two regions. Let its boundary be c_0 , minimum of the fitting energy (see in Fig. 3)

$$\text{Fit} = F_1(c_0) + F_2(c_0) = \inf \{F_1(C) + F_2(C)\} \approx 0. \quad (2)$$

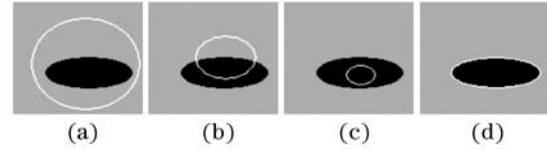


Fig. 3. Minimum of the fitting energy. (a) $F_1(C) > 0$, $F_2(C) \approx 0$, $\text{Fit}(C) > 0$; (b) $F_1(C) > 0$, $F_2(C) > 0$, $\text{Fit}(C) > 0$; (c) $F_1(C) \approx 0$, $F_2(C) > 0$, $\text{Fit}(C) > 0$; (d) $F_1(C) \approx 0$, $F_2(C) \approx 0$, $\text{Fit}(C) \approx 0$.

By adding two regularizing terms of the length of the curve C and the area inside curve C , the energy function is

$$\begin{aligned} F(C, c_1, c_2) &= \mu \cdot \text{length}(C) + \nu \cdot \text{area}(\text{inside}C) \\ &+ \lambda_1 \int_{\text{inside}(C)} |u_0 - c_1|^2 dx dy \\ &+ \lambda_2 \int_{\text{outside}(C)} |u_0 - c_2|^2 dx dy, \end{aligned} \quad (3)$$

where $\mu, \nu, \lambda_1, \lambda_2$ are fixed parameters.

In the level set method, a curve $C \subset \Omega$ is represented by the zero level set of a Lipschitz function $\phi : \Omega \rightarrow \mathfrak{R}$ (the Euclidean space of real number), such that

$$\begin{cases} C = \{(x, y) \in \Omega : \phi(x, y) = 0\} \\ \text{inside}(C) = \{(x, y) \in \Omega : \phi(x, y) > 0\} \\ \text{outside}(C) = \{(x, y) \in \Omega : \phi(x, y) < 0\} \end{cases}. \quad (4)$$

With the level set formulation in Ref. [6] the associated Euler-Lagrange equation is deduced

$$\begin{cases} \frac{\partial \phi(t, x, y)}{\partial t} = \delta_\varepsilon(\phi(x, y, t)) [\mu \text{div} \left(\frac{\nabla \phi(t, x, y)}{|\nabla \phi(t, x, y)|} \right) \\ \quad - \lambda_1 (u_0(x, y) - c_1)^2 + \lambda_2 (u_0(x, y) - c_2)^2] \\ \text{in } (0, +\infty) \times \Omega \\ \phi(0, x, y) = \phi_0(x, y) & \text{in } \Omega \\ \frac{\delta_\varepsilon(\phi)}{|\nabla \phi|} \frac{\partial \phi}{\partial \vec{n}} = 0 & \text{on } \partial \Omega \end{cases}, \quad (5)$$

where \vec{n} denotes the exterior normal to the boundary $\partial \Omega$, $\delta_\varepsilon(x)$ is the continuous approximation of Dirac delta function $\delta(x)$. The initial contour is defined as a curve $\phi_0(x, y) = 0$. Let $\phi(T, x, y)$ be the steady solution of Eq. (5), the boundary of the object to be detected is the curve $\phi(T, x, y) = 0$. Here the steady solution $\phi(T, x, y)$ means that if $t \geq T$, $\phi(t, x, y) = \phi(T, x, y)$. By the numerical discretization the numerical solution of the Eq. (5) can be solved with various stable finite difference schemes.

In this paper the associated Euler-Lagrange equation used in the detection of the flame front contour in a PLIF image is presented as follows

$$\begin{cases} \frac{\partial \phi(t, x, y)}{\partial t} = \delta_\varepsilon(\phi(x, y, t)) [\mu \text{div} \left(\frac{\nabla \phi(t, x, y)}{|\nabla \phi(t, x, y)|} \right) \\ \quad - \alpha (u_0(x, y) - c_1)^2 + (1 - \alpha) (u_0(x, y) - c_2)^2] \\ \text{in } (0, +\infty) \times \Omega \\ \phi(0, x, y) = \phi_0(x, y) & \text{in } \Omega \\ \frac{\delta_\varepsilon(\phi)}{|\nabla \phi|} \frac{\partial \phi}{\partial \vec{n}} = 0 & \text{on } \partial \Omega \end{cases}, \quad (6)$$

where $0 < \alpha < 1$ is a fixed parameter, Ω is the rectangle region of an image and $\partial \Omega$ is its boundary. The

corresponding energy function of Eq. (6) is

$$F(C, c_1, c_2) = \mu \cdot \text{length}(C) + \alpha \int_{\text{inside}(C)} |u_0 - c_1|^2 dx dy + (1 - \alpha) \int_{\text{outside}(C)} |u_0 - c_2|^2 dx dy. \quad (7)$$

Parameter α ($0 < \alpha < 1$) can be thought as the weighted factor of the contributions of the regions inside and outside curve C to the energy function. Choosing the value of the parameter depends on the distribution of intensities inside and outside the object. If in the object region the intensities are approximately constant and in the region outside the object the intensities vary greatly, α should be chosen as $0.5 < \alpha < 1$.

To discretize Eq. (6), the implicit finite difference scheme is used for the numerical solution of $\phi(t, x, y)$. The usual notations of the finite difference are at first presented: let h be the space step and Δt be the time step, and $(x_i, y_j) = (ih, jh)$ be the grid points for $1 \leq i \leq M$ and $1 \leq j \leq N$. Let $\phi_{i,j}^n = \phi(n\Delta t, x_i, y_j)$ be an approximation of $\phi(t, x, y)$ with $n \geq 0$, $\phi^0 = \phi_0$. The finite differences are

$$\begin{cases} \Delta_x^+ \phi_{i,j} = \phi_{i,j} - \phi_{i-1,j}, & \Delta_x^- \phi_{i,j} = \phi_{i,j} - \phi_{i+1,j} \\ \Delta_y^+ \phi_{i,j} = \phi_{i,j} - \phi_{i,j-1}, & \Delta_y^- \phi_{i,j} = \phi_{i,j} - \phi_{i,j+1} \\ \Delta_x^0 \phi_{i,j} = \phi_{i+1,j} - \phi_{i-1,j}, & \Delta_y^0 \phi_{i,j} = \phi_{i,j+1} - \phi_{i,j-1} \end{cases}.$$

The finite difference scheme is

$$\frac{\phi_{i,j}^{n+1} - \phi_{i,j}^n}{\Delta t} = \delta_h(\phi_{i,j}^n) \times \left[\frac{\mu}{h^2} \Delta_x^- \left(\frac{\Delta_x^+ \phi_{i,j}^{n+1}}{\sqrt{(\Delta_x^+ \phi_{i,j}^n)^2 / (h^2) + (\Delta_y^0 \phi_{i,j}^n)^2 / (2h)^2 + \tau}} \right) + \frac{\mu}{h^2} \Delta_y^- \left(\frac{\Delta_y^+ \phi_{i,j}^{n+1}}{\sqrt{(\Delta_x^0 \phi_{i,j}^n)^2 / (h^2) + (\Delta_y^+ \phi_{i,j}^n)^2 / (2h)^2 + \tau}} \right) - \alpha (u_{0,i,j} - c_1(\phi^n))^2 + (1 - \alpha) \cdot (u_{0,i,j} - c_2(\phi^n))^2 \right], \quad (8)$$

where $\Delta t = 0.2$, $\mu = 0.02 \times 255^2$ and $\tau = 0.000001$. For the numerical computation the parameter $\tau > 0$ is used to avoid the case that the denominators in Eq. (7) are zero. The scheme was proved to be stable. In the numerical computation the initial level set function $\phi_0(x, y)$ is chosen as

$$\phi_0(x, y) = r - \sqrt{(x - x_c)^2 + (y - y_c)^2}, \quad (9)$$

where $r > 0$ is a fixed parameter, and (x_c, y_c) is the center coordinates of a PLIF image. Usually in our numerical experiments $r = \min\{w/4, h/4\}$, where w is the width of a PLIF image and h is its height. The approximation of delta function is chosen as

$$\delta_h(x) = \frac{1}{1 + (\pi \cdot x)^2}. \quad (10)$$

The parameter μ is a scale parameter. If it is smaller, then smaller objects will be detected; if it is larger, then also only larger objects are detected^[6]. By a lot of numerical experiments with different μ values (from 0.001×255^2 to 0.1×255^2) the detected contours of flame fronts were almost same, and the larger μ makes the algorithm converge faster. The criterion of the steady solution for Eq. (8) used in this paper is that if $\max_{i,j} |\varphi_{i,j}^{n+1} - \varphi_{i,j}^n| < 0.05$, $\varphi_{i,j}^{n+1}$ is the steady solution of Eq. (8).

Figure 4 shows the evolution of level-set in a PLIF image. It is clear that as time increasing the curve approaches the flame edge and stops at the flame edge.

As tests with the different initial level set functions in a PLIF image, the final contours of flame fronts detected respectively are almost same (see in Fig. 5). The initial curve can be anywhere in an image and is not necessary to surround the object to be detected.

Figure 6 shows the results of the method for some images with different qualities. Even for the noisy images, the continuous boundary can also be extracted.

In conclusion, the active contour model without edge was used for automatic detection of flame fronts in PLIF

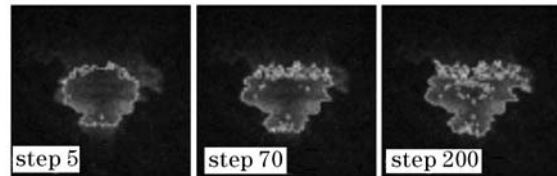


Fig. 4. Evolution of the zero level set.

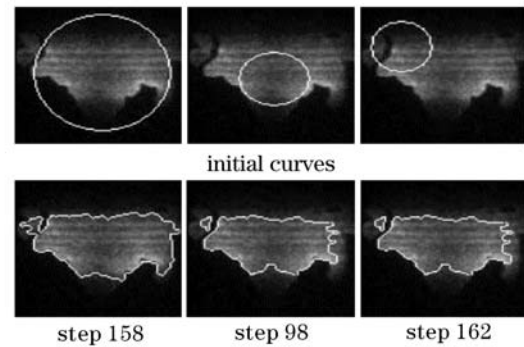


Fig. 5. Different initial level set functions and the almost same detected contours of flame front.

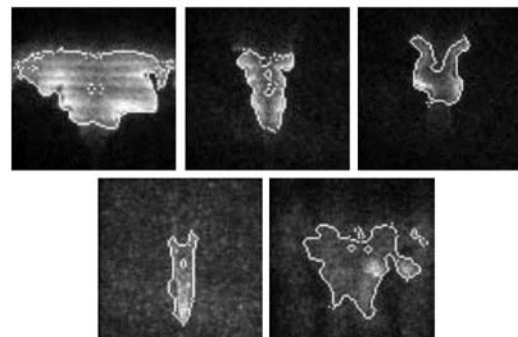


Fig. 6. Experiment results with different imaging qualities.

images. Because this model is not based on edge or some statistic information of an image, it is much more suitable and effective for automatic detection of flame fronts in large amounts of PLIF images. Another advantage is that the smoothing of initial image (or raw PLIF image) is not needed and the position of initial curve can be anywhere in an image. In this way the flame front is very well detected and preserved, even if it is very noisy image.

This work was partially supported by Natural Science Foundation of China under Grant No. 50276061. Y. Tang's e-mail address is ytang@sia.cn, Y. Wang's e-mail address is yuew@mail.etp.ac.cn, C. Eigenbrod's e-mail address is eigen@zarm.uni-bremen.de.

References

1. C. Eigenbrod, J. König, T. Bolik, H. Renken, and H. J. Rath, *Microgravity Sci. Technol.* **8**, (2) 134 (1995).
2. Y. Wang, J. König, and C. Eigenbrod, *Microgravity Sci. Technol.* **14**, (3) 25 (2003).
3. R. Abu-Gharbieh, G. Hamarneh, and T. Gustavsson, *Opt. Express* **8**, 278 (2001).
4. G. J. Smallwood, O. L. Gulder, D. R. Snelling, B. M. Deschamps, and I. Gokalp, *Combustion and Flame* **101**, 461 (1995).
5. R. Knikker, D. Veynante, J. C. Rolon, and C. Meneveau, in *Proceedings of the 10th international Symposium on Turbulence, Heat and Mass Transfer* (2000).
6. T. F. Chan and L. A. Vese, *IEEE Trans. Image Processing* **10**, 266 (2001).